

Comparison of periprosthetic femoral fracture torque and strain pattern of three types of femoral components in experimental model



**Y. Takegami,
T. Seki,
Y. Osawa,
S. Imagama**

From Nagoya University
Graduate School of
Medicine, Nagoya,
Japan

Aims

Periprosthetic hip fractures (PPFs) after total hip arthroplasty are difficult to treat. Therefore, it is important to identify modifiable risk factors such as stem selection to reduce the occurrence of PPFs. This study aimed to clarify differences in fracture torque, surface strain, and fracture type analysis between three different types of cemented stems.

Methods

We conducted biomechanical testing of bone analogues using six cemented stems of three different types: collarless polished tapered (CPT) stem, Versys Advocate (Versys) stem, and Charnley-Marcel-Kerboull (CMK) stem. Experienced surgeons implanted each of these types of stems into six bone analogues, and the analogues were compressed and internally rotated until failure. Torque to fracture and fracture type were recorded. We also measured surface strain distribution using triaxial rosettes.

Results

There was a significant difference in fracture torque between the three stem types ($p = 0.036$). Particularly, the median fracture torque for the CPT stem was significantly lower than that for the CMK stem (CPT vs CMK: 164.5 Nm vs 200.5 Nm; $p = 0.046$). The strain values for the CPT stem were higher than those for the other two stems at the most proximal site. The fracture pattern of the CPT and Versys stems was Vancouver type B, whereas that of the CMK stem was type C.

Conclusion

Our study suggested that the cobalt-chromium alloy material, polished surface finish, acute-square proximal form, and the absence of a collar may be associated with lower fracture torque, which may be related to PPF.

Cite this article: *Bone Joint Res* 2022;11(5):270–277.

Keywords: Periprosthetic femoral fractures, Biomechanical study, Fracture load, Stem design

Article focus

■ To decrease the risk of periprosthetic femoral fracture, the choice of stem is crucial. The purpose of this study was to clarify the differences in fracture torque, surface strain, and fracture type analysis between three different types of cemented stems in biomechanical study.

Key messages

■ The fracture torque of the femora with collarless polished tapered (CPT) stem was significantly lower than that of the femora with Charnley-Marcel-Kerboull (CMK) stem. The strain values for the CPT stem were higher than those for the other two stems at the most proximal site in the anterior and posterior of femur. The fracture pattern of the CPT and Versys stems

Correspondence should be sent to
Yasuhiko Takegami; email:
takegami@med.nagoya-u.ac.jp

doi: 10.1302/2046-3758.115.BJR-
2021-0375.R2

Bone Joint Res 2022;11(5):270–
277.

was Vancouver type B, whereas that of the CMK stem was Vancouver type C.

Strengths and limitations

- The strength of this study is that it clarified the difference in fracture torque between different stem concepts, and visualized the site of torque application by using a strain gauge.
- This model did not represent osteoporotic bone. We discarded the influence of the soft-tissue envelope in our model.

Introduction

The risk of periprosthetic fracture (PPF) after total hip arthroplasty is about 0.4% to 3.5%, which is relatively low,¹⁻³ yet PPFs are difficult to treat when they do occur. Prevention is likely to be a more effective strategy than treatment; thus the identification of modifiable risk factors that can guide surgical decision-making, such as the choice of stem, is crucial.

Several prior registry-based studies showed that the types of femoral stems and their fixation could be related to the increased risk of some prosthetic designs. The risk of fracture for the taper-slip stem was higher than that for the composite-beam stem.⁴ The use of a collarless polished tapered (CPT) stem was associated with the highest risk of revision for PPF compared with any of the other types of cemented stems.⁵

Among the several previous *in vitro* studies using the polished taper-slip stems, it was reported that torque to fracture was lower with a shorter stem than with a longer stem.⁶ Larger taper-slip stems with higher use rates are associated with greater torque to fracture.⁷ Femora implanted with the CPT stem showed that lower rotational force and torque were needed to generate PPF compared to femora implanted with the Exeter or DePuy C-Stem stems.⁸ Although compressive rotation tests using simulated bone and fracture type analysis have been performed in taper-slip type stems only, few studies have compared changes in fracture torque and fracture type between different stem concepts, including the composite-beam stem and the Charnley type stem.

The purpose of this study was to clarify the differences in fracture torque, surface strain, and fracture type analysis between three different types of cemented stems.

Methods

Materials. We prepared 18 bone analogues (Sawbones medium left femur model 3403; Pacific Research Laboratories, USA) for cemented implantation of the femoral components. These were divided into three groups of six each. We used The Optipac system (Zimmer Biomet, USA), which is already pre-packed with an identical amount and type of bone cement. The system contained 80 g of Refobacin Bone Cement R (Zimmer Biomet),

which was stored at ambient temperature, for filling in the Palamix and EasyMix systems.

Implants. We used three types of stems based on the new classification of cement stems described by Cassar-Gheiti et al⁹ (Figure 1). The CPT stem (Zimmer Biomet) is also known as a taper-slip or force-close stem. These stems are double-tapered without a collar, and the surface finish of these implants is polished. The Versys Advocate (Versys) stem (Zimmer Biomet) is known as a shape-closed or composite-beam type, which intends to maximize the interlock between the stem and the cement. The design of the stem is tapered and flanged with a collar, and its surface finish is satin. The Charnley-Marcel-Kerboull (CMK) stem (Zimmer Biomet) is designed to achieve a press-fit fixation in the anterior-posterior plane with a self-centering effect. The CMK stem has a polished surface with a collar.

Morishima et al⁶ showed that the difference in offset affected the difference in fracture torque. Therefore, in our study, we decided to unify the offsets among the stems to cancel the effect of offset. Table I shows the stem length and neck shaft angle of each stem when the offset was unified. We used the CT data of the composite femur. We planned the stem setting with 3D software (ZedHip LEXI, Japan). Using the template, we planned the head centre to be the same position for all stems.

Preparation. All implant constructs were prepared by an experienced orthopaedic surgeon (YT). According to the plan, we composed a plastic neck cutting guide, and the neck cut was performed accordingly. The bone analogues were broached using the appropriate broaching rasp for each stem. A bone plug made of wax was fixed into the femoral canal distal to the tip of the implant. The implant was then cemented without the use of a stem centralizer into the Sawbone using 80 g of Refobacin Bone Cement R (Zimmer Biomet).

Mechanical loading test. We conducted compression-torsion tests using a CMH Biaxial Material Test System (SAGINOMIYA SEISAKUSHO, Japan). This system allows the performance of a combination test with axial stress and torsional stress by adding biaxial forces to a test piece simultaneously. The phase between the forces can also be freely controlled. The proximal femur was held by a mechanical clamp at the centre of rotation of the implant head. We set the vertical loading axis of the machine through the centre of the femoral head and the intercondylar notch. The distal end of femur was fixed with special device (Figure 2). The femora were tested using combined compression force with torque to imitate fracture patterns in the femora. A preload of 2 Nm in the internal rotation direction and 2 kN of compression were applied as previously described.^{6,7} The compressive load was then maintained, and the implant was internally rotated 40° in one second. The angle of 40° was chosen to ensure that a fracture had fully occurred. Fracture torque was defined as the maximum torque measured. We recorded the fracture pattern in reference to the Vancouver classification.¹⁰

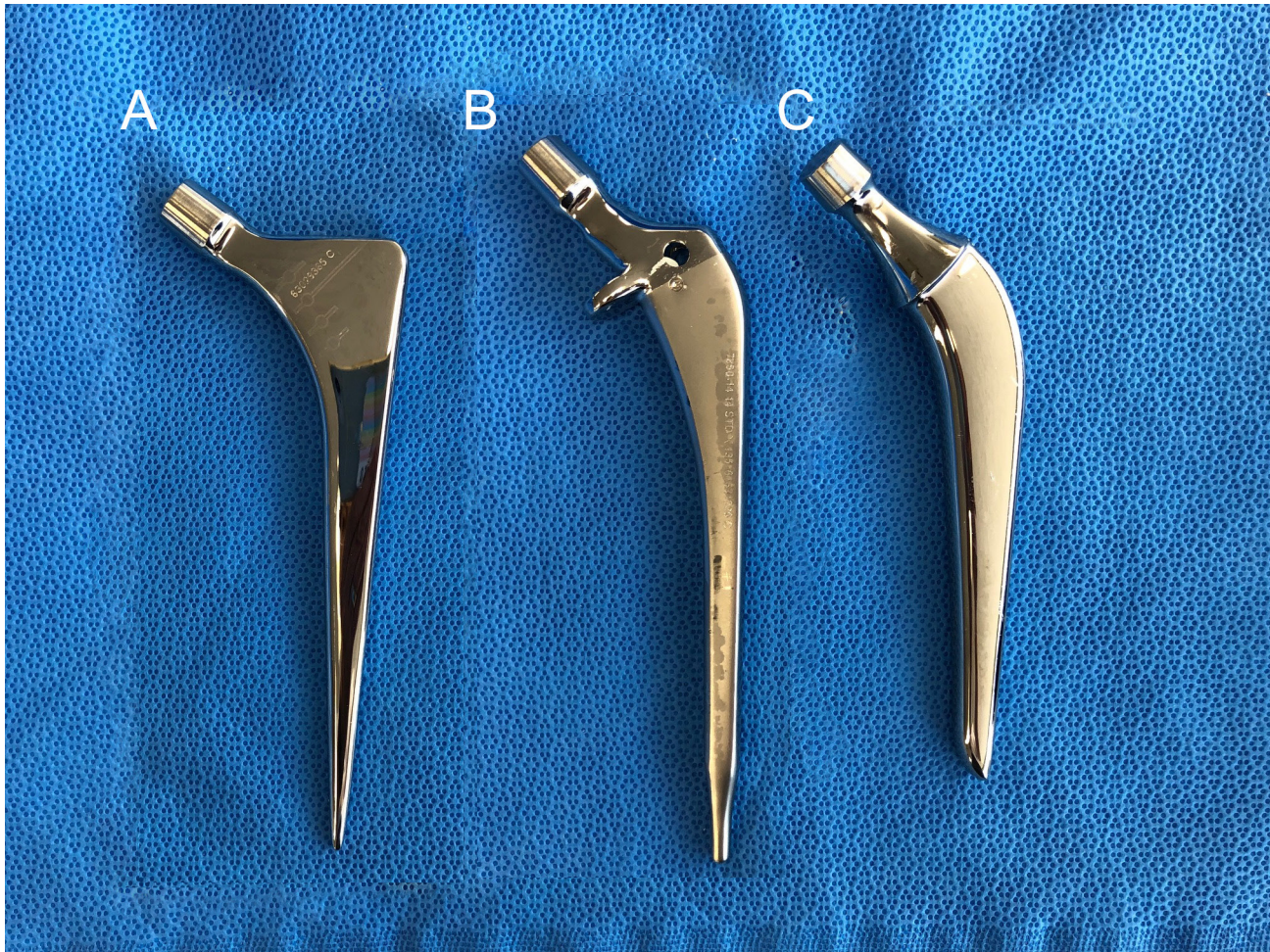


Fig. 1

a) The collarless polished tapered stem (Zimmer Biomet, USA), b) Versys Advocate (Zimmer Biomet), and c) Charnley-Marcel-Kerboull stem (Zimmer Biomet).

Table I. Implant size.

Variable	CPT stem	Versys Advocate stem	CMK stem
Manufacturer's stem size	3 (high offset)	14	203
Stem offset, mm	45	44	43
Neck length, mm	3.5	3.5	4
Total offset, mm	47.5	47.5	47
Stem length, mm	130	135	115
Neck shaft angle, °	125	135	130
Surface finish	Polished	Satin	Polished
Material	CoCr alloy	CoCr alloy	Stainless steel

CMK, Charnley-Marcel-Kerboull; CoCr, cobalt-chromium; CPT, collarless polished tapered.

Surface strain measurement. We measured surface strain distribution using triaxial rosettes (UFRA-5-350-17, Tokyo Sokki Kenkyujo, Japan) medially and laterally at the metaphyseal region according to a previous report.¹¹ The strain gauge positions on the femur surface were determined as in Figure 3a. The strain signal is measured from nine sections around the metaphyseal-diaphyseal region defined as follows: greater trochanter (Figure 3b: sections 1, 2, and 3), proximal medial calcar (Figure 3c: sections 4 and 5), anterior

(Figure 3d: sections 6 and 7), and posterior (Figure 3e: sections 8 and 9). We rasped a region larger than the bonding area using 220 to 320 grit carbide paper. The femur surface was then finely cleansed with a small amount of acetone. The adhesive (M-Bond 200 (Micro-Measurements, USA)) was then swabbed uniformly at the back of the strain gauge base. The strain gauge was attached to the femur surface and pressed down with mastic tape (M-M Number PCT-2 cellophane tape, Nitto Denko Corporation, Japan).



Fig. 2

The proximal femur is attached at the centre of rotation of the implant head by means of a clamp. The femoral head is located in the vertical loading axis of the machine, to replicate the natural loading axis of the femur.

A terminal foil shape connector (TF-2S) was placed near the gauge (3 to 5 mm) to support the wiring process. The gauge leads were soldered slightly taut to the connecting terminal to avoid excessive tension during strain measurement. The extension lead wire was soldered to the terminal wire at the opposite side of the connecting terminal. The terminal wires connected to the strain gauge were finally connected to a multichannel data logger (TDS-630, Tokyo Sokki Kenkyujo). The equivalent von Mises stress was calculated using the strain data acquired.

Statistical analysis. We used the Kruskal-Wallis test, followed by Bonferroni's post-hoc test, for fracture torque and strain distribution. A p-value of < 0.05 was considered to indicate statistical significance. The statistical analysis was performed with EZR (Saitama Medical Centre, Jichi Medical University, Japan).¹²

Results

Fracture torque. The median fracture torques were 164.5 Nm (interquartile range (IQR) 145.8 to 178.7) for the CPT stem, 171.5 Nm (IQR 153.0 to 180.2) for the Versys stem, and 200.5 Nm (IQR 193.8 to 208.0) for the CMK stem. There was a significant difference in fracture torque between the three types of stems ($p = 0.036$). The median fracture torque of the CPT stem in particular was significantly lower than that for the CMK stem ($p = 0.046$) (Figure 4).

Surface strain. Table II shows the maximum strain values for each stem. The median values statistically differed in

Sections 6 and 8 (proximal site both anterior and posterior). The differences in fracture strain values in the other sections were not statistically significant.

Fracture pattern. In all samples of the CPT stem (Figures 5a and 5b), the fracture spread from the posterior surface of the proximal femur to the diaphysis, and reached near the tip of the stem. The fractures were spirally shaped, and the degree of fracture comminution varied. We observed failure at the cement-bone interface in all cases. In the samples of the Versys stem (Figures 5c and 5d), the fractures occurred vertically, running from the cut to the diaphysis from the medial side of the greater trochanter posteriorly, and from the base of the collar anteriorly. The fragments were larger than those in the CPT stem fractures. The CMK stem (Figures 5e and 5f) showed a comminuted oblique fracture of Vancouver type C at the tip of the stem in all cases.

Discussion

This biomechanical study showed that torque to fracture was significantly different depending on the stem concepts, and that the fracture torque of the femora with CPT stem in particular was significantly lower than that of the femora with CMK stem. The strain values statistically differed in the proximal site, both anteriorly and posteriorly, depending on the types of stems. The fracture pattern of the CPT and Versys stems was Vancouver type B, whereas that of the CMK stem was Vancouver type C.

The CPT had significantly lower fracture torque than the CMK; Versys had no significant difference with either stem. This could be attributed to the material and the surface finish: CPT is a cobalt-chromium alloy (CoCr) stem with a polished finish; Versys is a CoCr stem but with a satin finish; and CMK is stainless steel with a polished finish.

In a biomechanical study comparing three different types of tapered slip-type stems, they reported that PPF occurred in CPT implanted femora at lower torque forces compared with those implanted with the Exeter or DePuy C-Stem stems. The surface finish of all three stems is polished, but the CPT is made by CoCr, while the Exeter and C stems are stainless steel stems.⁸ Surface wettability of materials is related to metal fixation in bone cement. Borruto et al¹³ showed that different surface wettability between materials affects the coefficient of friction between cement and implant. Another biomechanical study revealed the difference of the hydrophobic nature between the metal materials, including CoCr and stainless steel.¹⁴ The study showed that CoCr had a lower surface wettability than stainless steel, and tended not to adhere to bone cement with a polished surface. Furthermore, the frictional coefficient of CoCr was significantly lower than that of stainless steel.¹⁴ These results indicate that, in CoCr, the low adhesion effect with low frictional coefficient may result in the excessive taper-slip. Tsuda¹⁵ demonstrated that subsidence into the bone cement was significantly greater in

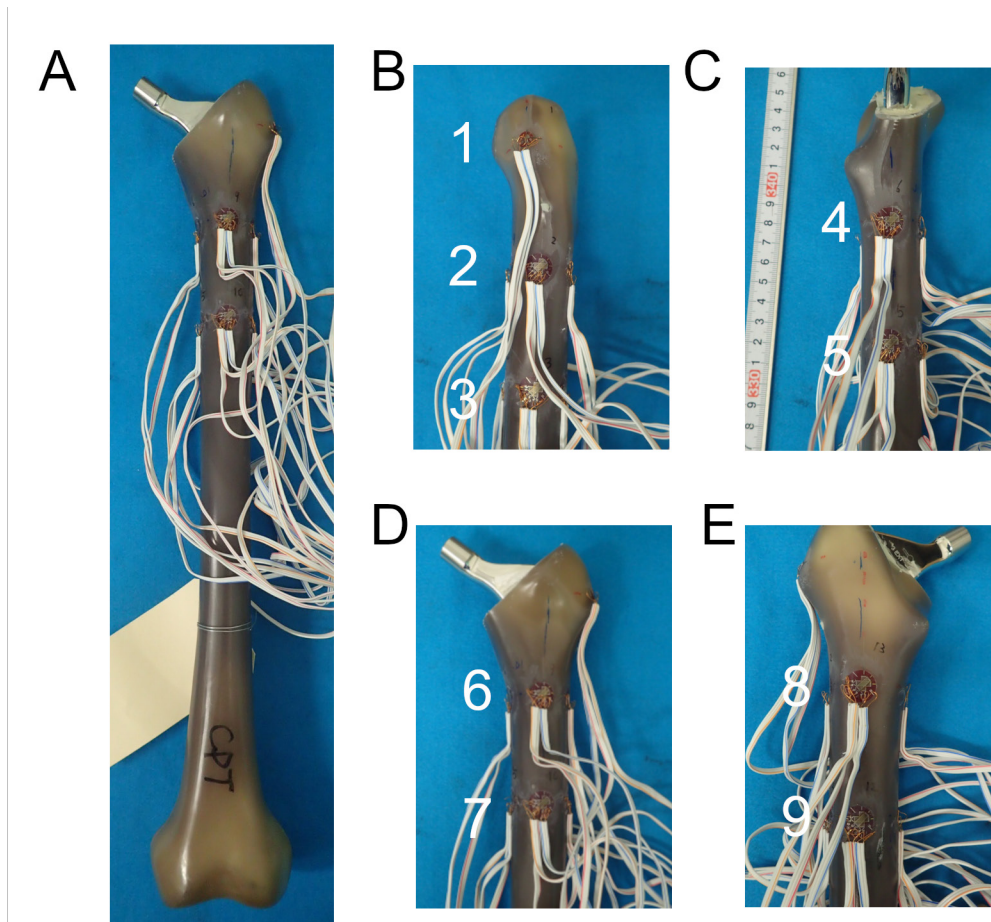


Fig. 3

a) The bone analogue with sensors attached. b) to e) Location of the strain sensors. b) Lateral (1, 2, and 3), c) medial (4 and 5), d) anterior (6 and 7), and e) posterior (8 and 9).

CoCr stem than in stainless steel stem. They speculated that the difference of surface wettability between the two materials is associated with the different mechanical behaviours in the bone cement. Lamb et al¹⁶ also showed, through their study of data from the National Joint Registry, that CoCr stems were associated with a higher risk of PFF compared with stainless steel stems, regardless of cement viscosity. These results suggest that the material difference in polished taper stem may affect subsidence in the cement.

The surface appearance also depended on the wettability of each metal. Hirata et al¹⁴ demonstrated that the decreasing surface roughness increased the contact angle, and that metal surface wettability decreased in accordance with greater polishing. In addition, regardless of the metal type, the roughness of the surface finish is proportional to the coefficient of friction. When the surface finish was satin, the friction coefficient was about twice that of polished finish.¹⁴ The surface design would matter, as roughness would create interlocking at the

cement implant interface. This would in turn change the biomechanical properties of stem at the interface.¹⁵

In the proximal femur, the three types of stems showed different surface strains, and although not significant, the CPT was more strained than the CMK. This may be related to the cross-sectional shape of the proximal stem design, and the presence of the collar. The cross-sectional shape of the stem is a triple-tapered design with CPT being the most acute and square, whereas Versys has a less acute and square design and CMK has a more rounded shape. Windell et al⁸ also showed that the implant shape is one of the biomechanical features of implants that could affect their behaviour in loading test to the point of failure. We assumed that the various stem shapes caused differences in proximal surface strain, resulting in differences in fracture type.

In our results, the distortion of the bone surface was smaller in the stem with the collar than in the collar-less stem. In a previous biomechanical study, the stem collar works protectively against subsidence. Total mean subsidence of the cemented stem in the calcar-collar contact group was significantly less than that in the

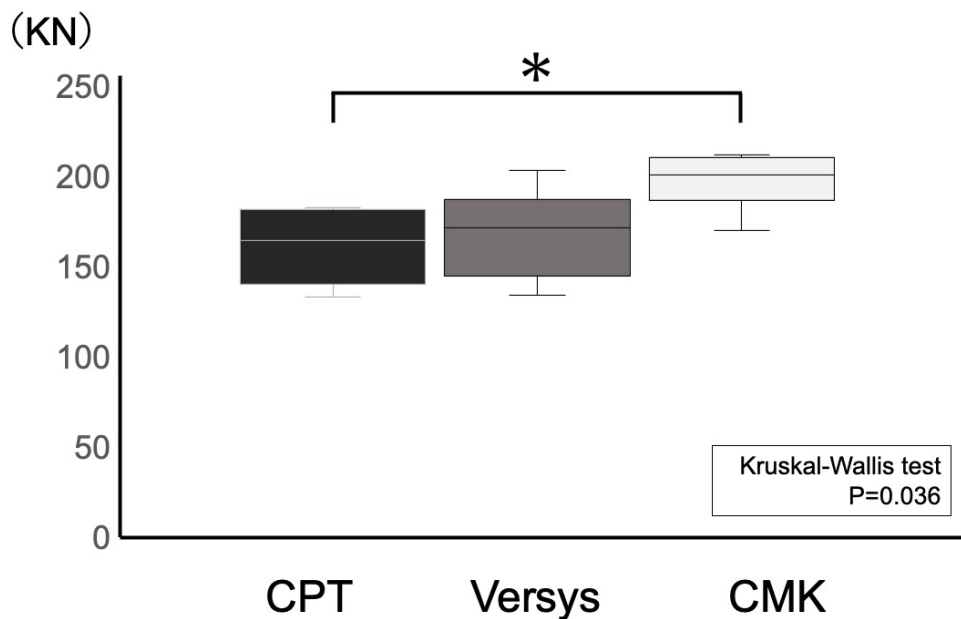


Fig. 4

The fracture torque between the three stems: collarless polished tapered (CPT), Versys Advocate, and Charnley-Marcel-Kerboull (CMK). Values for fracture torque are presented as box plots, where each box represents the 25th and 75th percentiles, the line within the box represents the median, and the whisker bars represent the 10th and 90th percentiles. *p-value < 0.05 for post hoc analysis.

Table II. Median maximum strain of each stem (interquartile range). All p-values were calculated using Kruskal-Wallis test.

Stem	Stem section								
	1	2	3	4	5	6	7	8	9
CPT, $\mu\epsilon$	379 (350 to 401)	2,841 (2,820 to 2,979.5)	5,587 (5,557 to 5,632.5)	4,445 (4,411.5 to 732.5)	2,956 (2,904 to 2,972.5)	3,501 (3,283 to 3,565.5)	5,532 (5,467.5 to 5,544.5)	5,232 (5,220.5 to 5,277.5)	4,226 (3,882.5 to 4,725.5)
Versys, $\mu\epsilon$	172 (169.5 to 214)	2,160 (2,129 to 2,342)	5,146 (4,924.5 to 5,613)	4,485 (4,123 to 4,677.5)	2,267 (2,132 to 2,442)	2,694 (2,675 to 2,731)	4,446 (4,432.5 to 4,546.5)	5,156 (5,140.5 to 5,214.5)	3,954 (3,663 to 3,979)
CMK, $\mu\epsilon$	181 (175.5 to 198)	2,645 (2,298 to 2,886)	4,937 (4,879.5 to 5,569)	4,600 (4,676.5 to 4,895)	2,882 (2,807.5 to 3,040.5)	2,946 (2,852.5 to 3,046.5)	4,355 (4,473.5 to 4,689)	4,903 (4,892.5 to 4,999)	4,565 (4,460 to 4,679)
p-value	0.067	0.148	0.733	0.561	0.067	0.048	0.067	0.048	0.148

CMK, Charnley-Marcel-Kerboull; CPT, collarless polished tapered.

non-calcus-collar contact group (0.38 mm vs 0.80 mm, $p = 0.002$).¹⁷ Even in the cementless stem, the fracture torque and torsional stiffness in the calcus-collar contact group are greater than those in the non-contact group.^{16,18}

These results indicate that the collar would work defensively against excessive sinking. We speculated that stem material, surface finish, and the presence of a collar would be associated with excessive stem subsidence, which may be related to PPF.

In the present study, a Vancouver type B2 fracture occurred in the composite femora with the CPT and Versys stems, whereas a type C fracture occurred in the composite femora with the CMK stem. The fractures were most comminuted with the CPT stem. The experiments of Morishima et al⁶ and Ginsel et al⁷ also resulted

in type B fractures. Chatzigorou et al¹⁹ revealed that the Exeter, which is a polished stem, had a higher risk of type B fracture. Conversely, the Lubinus SPII, which is a shape-closed anatomically S-shaped stem with collar, had comminuted fractures located distally to the stem.

The CMK stem, which is the shortest in length, produced the greatest fracture torque. There are several reports that suggest longer stems are better. Morishima et al⁶ showed that a femur with a short stem could be broken with less torque, and Kwak et al²⁰ reported that in terms of stress distribution at the cortical bone around the femoral stem, the longest stem was least likely to break; this is corroborated by Windell et al.⁸ All of these studies compared taper-slip types of the same design, so stem design may have a greater effect on breaking torque than stem length.

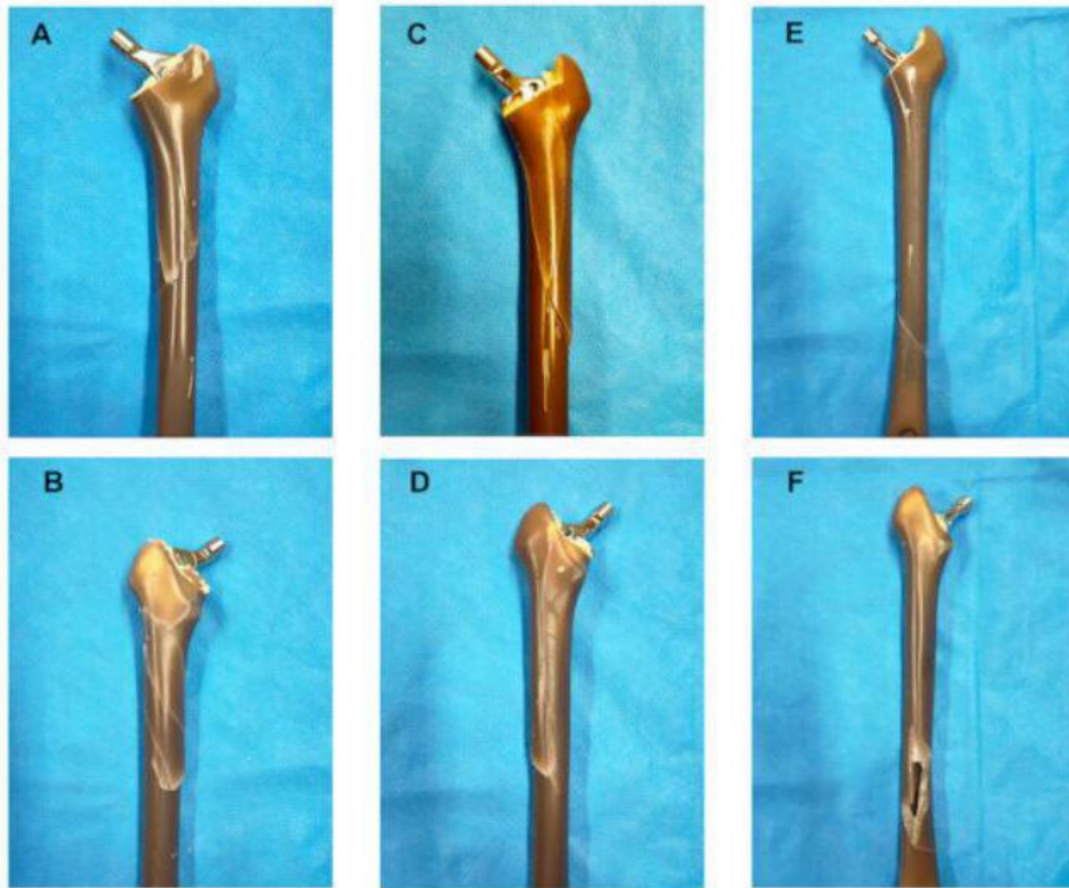


Fig. 5

Examples of the fracture pattern of each stem created by our testing mechanism. a) and b) Collarless polished tapered stem: a) anterior side, b) posterior side. c) and d) Versys stem: c) anterior side, d) posterior side. e) and f) Charnley-Marcel-Kerboull stem: e) anterior side, f) posterior side.

The present study has several limitations. First, we used a bone analogue, which represents a normal femoral bone in a healthy young male, and not an osteoporotic bone model. This model was used because at the time of testing there was no validated bone analogue available for osteoporotic bone, and cadaveric bone was not available. PPFs of the femur often occur in elderly patients;²¹ we predict that an osteoporotic model would show a lower-energy fracture. Second, we discarded the influence of the soft-tissue envelope in our model. In an in vivo model, several muscle groups would counter the internal torsion force applied in the model. This would potentially influence the direction of force and the fracture pattern. Third, we considered three different types of stems but not all types of cement stems. Fourth, we only showed the fracture torque of compressive torsion, not other mechanisms such as torsion, bending, and direct impact.

In conclusion, our study suggested that the CoCr alloy material, polished surface finish, acute-square proximal

form, and the absence of a collar may be associated with lower fracture torque, which may be related to PPF. The difference of surface strain pattern may be associated with the difference of fracture pattern.

References

1. Patsiogiannis N, Kanakaris NK, Giannoudis PV. Periprosthetic hip fractures: an update into their management and clinical outcomes. *EFORT Open Rev.* 2021;6(1):75–92.
2. Abdel MP, Watts CD, Houdek MT, Lewallen DG, Berry DJ. Epidemiology of periprosthetic fracture of the femur in 32 644 primary total hip arthroplasties: a 40-year experience. *Bone Joint J.* 2016;98-B(4):461–467.
3. Lindahl H. Epidemiology of periprosthetic femur fracture around a total hip arthroplasty. *Injury.* 2007;38(6):651–654.
4. Thien TM, Chatziagorou G, Garellick G, et al. Periprosthetic femoral fracture within two years after total hip replacement: analysis of 437,629 operations in the nordic arthroplasty register association database. *J Bone Joint Surg Am.* 2014;96-A(19):e167.
5. Palan J, Smith MC, Gregg P, et al. The influence of cemented femoral stem choice on the incidence of revision for periprosthetic fracture after primary total hip arthroplasty: an analysis of national joint registry data. *Bone Joint J.* 2016;98-B(10):1347–1354.

6. **Morishima T, Ginsel BL, Choy GGH, Wilson LJ, Whitehouse SL, Crawford RW.** Periprosthetic fracture torque for short versus standard cemented hip stems: an experimental in vitro study. *J Arthroplasty.* 2014;29(5):1067–1071.
7. **Ginsel BL, Morishima T, Wilson LJ, Whitehouse SL, Crawford RW.** Can larger-bodied cemented femoral components reduce periprosthetic fractures? A biomechanical study. *Arch Orthop Trauma Surg.* 2015;135(4):517–522.
8. **Windell L, Kulkarni A, Alabort E, Barba D, Reed R, Singh HP.** Biomechanical comparison of periprosthetic femoral fracture risk in three femoral components in a sawbone model. *J Arthroplasty.* 2021;36(1):387–394.
9. **Cassar-Gheiti AJ, McColgan R, Kelly M, Cassar-Gheiti TM, Kenny P, Murphy CG.** Current concepts and outcomes in cemented femoral stem design and cementation techniques: the argument for a new classification system. *EFORT Open Rev.* 2020;5(4):241–252.
10. **Brady OH, Garbuz DS, Masri BA, Duncan CP.** The reliability and validity of the Vancouver classification of femoral fractures after hip replacement. *J Arthroplasty.* 2000;15(1):59–62.
11. **Baharuddin MY, Salleh S-H, Hamed M, et al.** Primary stability recognition of the newly designed cementless femoral stem using digital signal processing. *Biomed Res Int.* 2014;2014:478248.
12. **Kanda Y.** Investigation of the freely available easy-to-use software “EZR” for medical statistics. *Bone Marrow Transplant.* 2013;48(3):452–458.
13. **Borruto A, Crivellone G, Marani F.** Influence of surface wettability on friction and wear tests. *Wear.* 1998;222(1):57–65.
14. **Hirata M, Oe K, Kaneuji A, Uozu R, Shintani K, Saito T.** Relationship between the surface roughness of material and bone cement: an increased “polished” stem may result in the excessive taper-slip. *Materials (Basel).* 2021;14(13):3702.
15. **Tsuda R.** [Differences in mechanical behavior between Cobalt-chrome alloy and stainless-steel alloy in polished tapered femoral stems fixed with bone cement]. *J Kanazawa Med Univ.* 2016;41:1–9. [Article in Japanese].
16. **Lamb JN, Baetz J, Messer-Hannemann P, et al.** A calcar collar is protective against early periprosthetic femoral fracture around cementless femoral components in primary total hip arthroplasty: a registry study with biomechanical validation. *Bone Joint J.* 2019;101-B(7):779–786.
17. **Numata Y, Kaneuji A, Kerboul L, et al.** Biomechanical behaviour of a French femoral component with thin cement mantle: The “French paradox” may not be a paradox after all. *Bone Joint Res.* 2018;7(7):485–493.
18. **Lamb JN, Coltart O, Adekanmbi I, Pandit HG, Stewart T.** Calcar-collar contact during simulated periprosthetic femoral fractures increases resistance to fracture and depends on the initial separation on implantation: A composite femur in vitro study. *Clin Biomech (Bristol, Avon).* 2021;87:105411.
19. **Chatziagorou G, Lindahl H, Kärrholm J.** The design of the cemented stem influences the risk of Vancouver type B fractures, but not of type C: an analysis of 82,837 Lubinus SPII and Exeter Polished stems. *Acta Orthop.* 2019;90(2):135–142.
20. **Kwak DK, Bang SH, Lee SJ, Park JH, Yoo JH.** Effect of stem position and length on bone-stem constructs after cementless hip arthroplasty. *Bone Joint Res.* 2021;10(4):250–258.
21. **Brodén C, Mukka S, Muren O, et al.** High risk of early periprosthetic fractures after primary hip arthroplasty in elderly patients using a cemented, tapered, polished stem. *Acta Orthop.* 2015;86(2):169–174.

Author information:

- Y. Takegami, MD, PhD, Lecturer
- T. Seki, MD, PhD, Assistant Professor
- Y. Osawa, MD, PhD, Clinical Fellow
- S. Imagama, MD, PhD, Professor
Department of Orthopaedic Surgery, Nagoya University Graduate School of Medicine, Nagoya, Japan.

Author contributions:

- Y. Takegami: Conceptualization, Methodology, Writing – original draft, Writing – review & editing.
- T. Seki: Conceptualization.
- Y. Osawa: Formal analysis, Investigation.
- S. Imagama: Resources, Supervision.

Funding statement:

- The authors disclose receipt of the following financial or material support for the research, authorship, and/or publication of this article: Zimmer Biomet provided the authors with the stems and cement for this study.

Acknowledgements:

- We would like to express our deepest gratitude to NIPPON STEEL TECHNOLOGY Co., Ltd. for helping to measure the fracture torque and strain.

Open access funding

- The authors confirm that the open access fee for this study was self-funded.

© 2022 Author(s) et al. This is an open-access article distributed under the terms of the Creative Commons Attribution Non-Commercial No Derivatives (CC BY-NC-ND 4.0) licence, which permits the copying and redistribution of the work only, and provided the original author and source are credited. See <https://creativecommons.org/licenses/by-nc-nd/4.0/>